N73-11891

NASA TECHNICAL MEMORANDUM

NASA TM X-2667

NASA TM X-2667

WIND-TUNNEL TESTS OF A SINGLE-STAGE-TO-ORBIT SPACE SHUTTLE AT MACH NUMBERS OF 2.60, 3.85, AND 4.64

by Ernald B. Graves

Langley Research Center
Hampton, Va. 23365

NATIONAL AERONAUTICS AND SPACE ADMINISTRATION • WASHINGTON, D. C. • NOVEMBER 1972

1. Report No. NASA TM X-2667	2. Government Accession No.	3. Recipient's Catalog No.
4. Title and Subtitle WIND-TUNNEL TESTS OF A SINGLE-STAGE-TO-ORBIT SPACE SHUTTLE AT MACH NUMBERS OF 2.60, 3.85, AND 4.64		5. Report Date November 1972
		6. Performing Organization Code
7. Author(s) Ernald B. Graves		8. Performing Organization Report No. L-8480
		10. Work Unit No. 502-37-01-01
9. Performing Organization Name and Address NASA Langley Research Center Hampton, Va. 23365		11. Contract or Grant No.
		13. Type of Report and Period Covered Technical Memorandum
12. Sponsoring Agency Name and Address National Aeronautics and Space Administration Washington, D.C. 20546		14. Sponsoring Agency Code
15. Supplementary Notes		

16. Abstract

Tests have been conducted in the Langley Unitary Plan wind tunnel to determine the static aerodynamic characteristics of a single-stage-to-orbit space shuttle model at Mach numbers of 2.60, 3.85, and 4.64. Test parameters included various payloads for the launch configurations and various corner radii for the entry configurations.

The test results for the launch configurations generally indicated that a decrease in payload size resulted in a marked increase in axial force. Decreasing the corner radii of the entry configuration led to large increases in axial force. The results also indicated that the presence of an engine door on the entry configuration caused a measurable positive increment in pitching moment. Changing the entry configuration afterbody geometry from a biconic shape to a conic shape increased the normal-force and stability level.

17. Key Words (Suggested by Author(s))	18. Distribution Statement
Space shuttle Reentry Biconic configuration	Unclassified – Unlimited

19. Security Classif. (of this report)	20. Security Classif. (of this page)	21. No. of Pages	22. Price*
Unclassified	Unclassified	28	$3.00

*For sale by the National Technical Information Service, Springfield, Virginia 22151

WIND-TUNNEL TESTS OF A SINGLE-STAGE-TO-ORBIT SPACE SHUTTLE AT MACH NUMBERS OF 2.60, 3.85, AND 4.64

By Ernald B. Graves
Langley Research Center

SUMMARY

Tests have been conducted in the Langley Unitary Plan wind tunnel to determine the static aerodynamic characteristics of a single-stage-to-orbit space shuttle model at Mach numbers of 2.60, 3.85, and 4.64. Test parameters included various payloads for the launch configurations and various corner radii for the entry configurations.

The test results for the launch configurations generally indicated that a decrease in payload size resulted in a marked increase in axial force. Decreasing the corner radii of the entry configuration led to large increases in axial force. The results also indicated that the presence of an engine door on the entry configuration caused a measurable positive increment in pitching moment. Changing the entry configuration afterbody geometry from a biconic shape to a conic shape increased the normal-force and stability level.

INTRODUCTION

The National Aeronautics and Space Administration is currently engaged in studies directed toward the development of a low-cost reusable space shuttle system capable of earth orbit. One design concept under investigation is a single-stage-to-orbit vehicle. The concept consists of a large biconic body with a payload mounted at the apex. By design the body is essentially a large fuel tank with an aerospike rocket engine mounted in the base and extending around the complete periphery. During launch, the engine is exposed by opening numerous doors forming the corner of the blunt base (heat shield). Thrust from the engine places the payload and body in earth orbit. After the payload has been ejected, the body makes a ballistic reentry, the heat shield entering first. On the terminal descent phase of the flight, additional doors open in the heat shield to expose airbreathing direct lift engines and a vertical soft landing is made. As a part of the conceptual study, tests were performed in the Langley Unitary Plan wind tunnel on several 0.0055-scale models of launch and entry configurations. The tests, which were conducted at Mach numbers of 2.60, 3.85, and 4.64, were performed to determine the static aerodynamic characteristics for the launch configuration with various payloads and for the entry configuration with various corner radii.

SYMBOLS

The aerodynamic coefficients are referenced to the body-axis system. The moment reference for all test configurations is at model station 0.00 (see fig. 1) which is on the face of the heat shield for the design concept. The measurements and calculations were made in U.S. Customary Units. Values are given in SI Units and parenthetically in U.S. Customary Units. The symbols are defined as follows:

C_A axial-force coefficient, $\frac{\text{Axial force}}{qS}$

$C_{A,b}$ base axial-force coefficient, $\frac{\text{Base axial force}}{qS}$

C_m pitching-moment coefficient, $\frac{\text{Pitching moment}}{qS}$

C_{m_α} pitching-moment-curve slope, per deg

C_N normal-force coefficient, $\frac{\text{Normal force}}{qS}$

C_{N_α} normal-force-curve slope, per deg

d reference diameter, 15.24 cm (6.00 in.)

M free-stream Mach number

q free-stream dynamic pressure, N/m^2 (lb/ft^2)

r_b radius of curvature of heat-shield face

r_c radius of curvature of engine-door corner

S reference area (based on d), 0.01824 m^2 (0.1963 ft^2)

α angle of attack, deg

Model nomenclature:

B_1 $45^\circ/25^\circ$ frustum baseline ascent body with balance cavity on center line

B_3	$45^{\circ}/25^{\circ}$ frustum baseline descent body with balance cavity rotated 16°
B_5	25° frustum descent body with balance cavity on center line
D_2	11-percent corner radius with engine doors open 25°
D_3	11-percent corner radius with engine doors open 45°
D_4	11-percent corner radius with engine doors closed
D_5	5-percent corner radius with engine doors closed
D_6	engine doors removed
D_8	differential corner radii: 5 percent for upper quadrant and 11 percent for lower quadrant with engine doors closed
F_1	large body of revolution payload, 5.59 cm (2.2 in.) maximum diameter
F_2	long body of revolution payload, 3.81 cm (1.5 in.) maximum diameter
F_3	winged payload, 3.15 cm (1.24 in.) maximum span
F_4	short body of revolution payload, 3.81 cm (1.5 in.) maximum diameter
O	entry configuration with no afterbody payload attached

APPARATUS AND METHODS

Tunnel

The investigation was conducted in the high Mach number test section of the Langley Unitary Plan wind tunnel which is a variable-pressure continuous-flow facility. The test section is about 1.22 meters (4 ft) square and 2.13 meters (7 ft) long. The nozzle leading to the test section is of the asymmetric sliding block type which permits a continuous variation in Mach number from about 2.3 to 4.7.

Model

Sketches of the test configuration are shown in figure 1. Photographs of some of the configurations are presented as figure 2.

Launch configurations.- The launch configurations consisted of a biconic $45^{\circ}/25^{\circ}$ body (B_1) with payload forebodies consisting of several bodies of revolution and a winged payload (F_1 to F_4). The engine doors which formed the periphery or "corner" of the base were simulated open at 25° (D_2) or 45° (D_3) by solid rings. The gaps between the numerous doors which would be required on an actual vehicle were not simulated and the heat-shield base that would exist inside of the ring was omitted to facilitate model balance installation.

Entry configurations.- The entry configurations (O) were tested with a simulated heat shield forward (integral with the engine door), with engine doors closed, and had no payloads attached. Engine door variations consisted of D_4 with 11-percent corner radius, D_5 with 5-percent corner radius, D_6 with engine doors removed, and D_8 with 5-percent upper corner radius and 11-percent lower corner radius. (See fig. 1.) An entry configuration with 25° conic afterbody (B_5) was also provided and was used with the D_4 door. Entry configurations 6 to 9 had an asymmetrical aft section to facilitate an increase in the positive angle-of-attack range. It should be noted that because of the difference in the D_5 corner radii, the heat-shield face does not encompass model station 0.00, the moment reference location.

Test Conditions

The tests were performed at Mach numbers of 2.60, 3.85, and 4.64 at a constant Reynolds number of 9.84×10^6 per meter (3×10^6 per foot). The test-section stagnation temperature was 338.7 K (150° F) at $M = 2.60$ and 352.6 K (176° F) at $M = 3.85$ and $M = 4.64$. The dewpoint temperature in the test section was maintained sufficiently low to insure negligible condensation effects.

Transition strips of no. 40 sand grit were placed 3.05 cm (1.2 in.) aft of the payload nose for launch configurations 1, 2, 4, and 5. The launch configuration winged payload and all entry configurations were tested transition free.

Measurements and Corrections

Forces and moments on the model were measured by means of an internally mounted three-component electrical strain-gage balance which, in turn, was rigidly fastened to a sting-support system. Pressures were measured in the balance chamber by means of a single static orifice.

Angles of attack have been corrected for sting-balance deflection due to model aerodynamic loads and for tunnel airflow misalinement. The axial-force coefficients for the launch configurations have been adjusted to free-stream static conditions acting over the base of the model. No axial-force adjustments have been made to the data for the entry configurations. Base axial-force coefficients are presented in figure 3.

DISCUSSION

Data for the launch configurations tested are presented in figure 4. The effect of payload size is seen by comparing the data for configurations 1, 2, and 4. These data indicate that decreasing payload size leads to a slight decrease in C_{m_α} and C_{N_α}. Of much greater significance, however, is the large increase in axial force with decrease in payload size. This effect may be explained by examining the flow field patterns shown in the schlieren photographs of figure 5. For configuration 1 the shock pattern from the large payload separates the flow forward of the body so that only a small part of the body is affected by the bow wave usually associated with blunt bodies of this type. The payload of configuration 2 has a smaller diameter coupled with a shorter length, and the shock wave from this payload results in a greater part of the body being influenced by the body bow wave. The small payload of configuration 4 results in the body being almost totally influenced by the blunt body bow wave. Configuration 3 with its small winged payload is also strongly influenced by the body bow wave and results in relatively large axial-force values. The data in figure 4 indicate little effect of door geometry on the aerodynamic characteristics of the vehicle (configurations 2 and 5).

The entry configuration data are presented in figure 6. Relatively linear pitching-moment and normal-force variations with angle of attack are indicated for all configurations. The effect of heat-shield corner radius is seen by comparing the data of configurations 6 (11-percent radius) and 7 (5-percent radius). Decreasing the corner radius leads to a slight decrease in C_{N_α} with only small effects on the pitching-moment coefficient. There is, however, a significant increase in axial force with decrease in corner radius throughout the entire angle-of-attack and Mach number range.

The differential corner radius model (configuration 9) incorporated a combination of the two radii (5-percent radii at the top, 11-percent radii at the bottom). This asymmetric model geometry induces a positive increment in pitching moment along with axial-force values that are essentially the same as those for configuration 7 (symmetrical 5-percent radius). It should be noted that these tests were performed with transition-free models and the results might be somewhat different for the full-scale vehicle in flight.

Configuration 8 simulates the vehicle with the engine door removed. With the door removed, there is a noticeable negative increment in pitching moment when compared with the other configurations. The axial force for this model is also generally less than those for the other entry models tested. A change in the entry afterbody from a biconic ($45^{\circ}/25^{\circ}$) geometry to a straight conic (25°) geometry produces little change in axial force but leads to an increase in $C_{N_{\alpha}}$ and stability level.

CONCLUSIONS

Results of tests to determine the static aerodynamic characteristics of a single-stage-to-orbit space shuttle vehicle at Mach numbers of 2.60, 3.85, and 4.64 have led to the following conclusions:

1. A decrease in launch configuration payload size generally led to a marked increase in axial force.

2. A decrease in entry configuration corner radii led to large increases in axial force.

3. An engine door on the entry configuration caused a measurable positive increment in pitching moment.

4. A change in entry configuration afterbody geometry from a biconic shape to a conic shape increased the normal-force and stability level.

Langley Research Center,
National Aeronautics and Space Administration,
Hampton, Va., October 26, 1972.

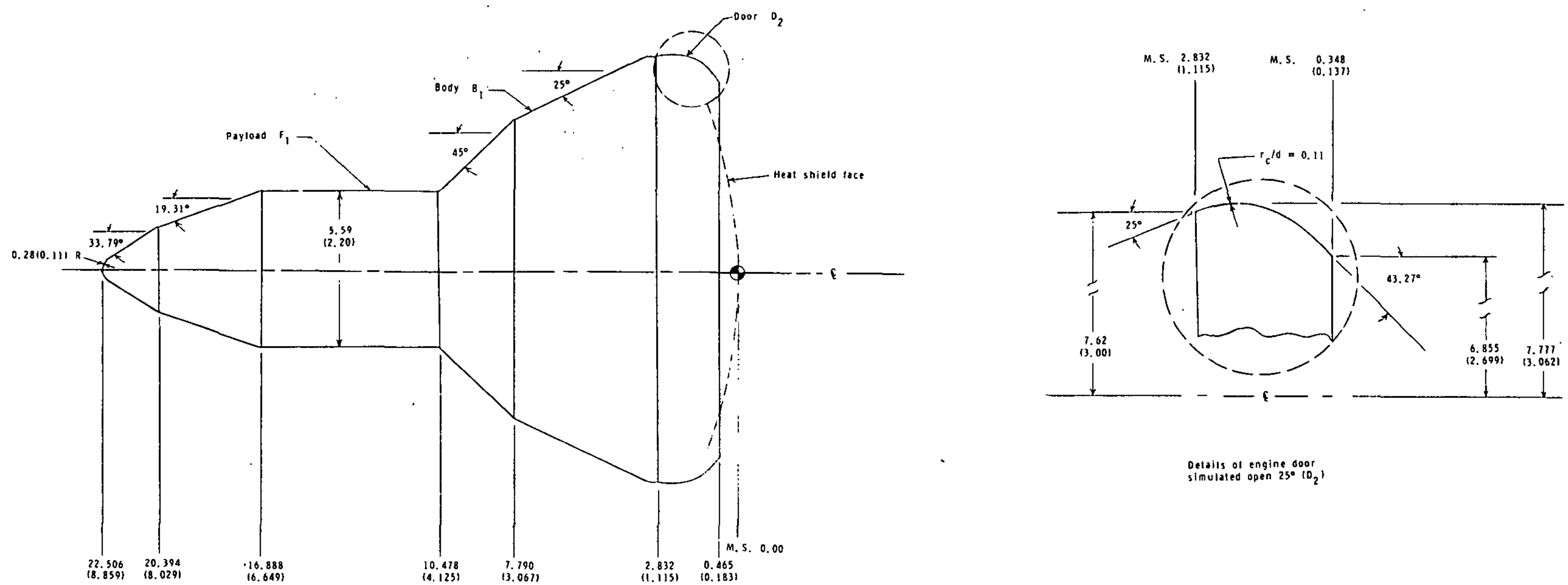

(a) Configuration 1 ($F_1B_1D_2$).

Figure 1.- Sketches of test configurations. All model stations (M.S.) are given in centimeters (inches).

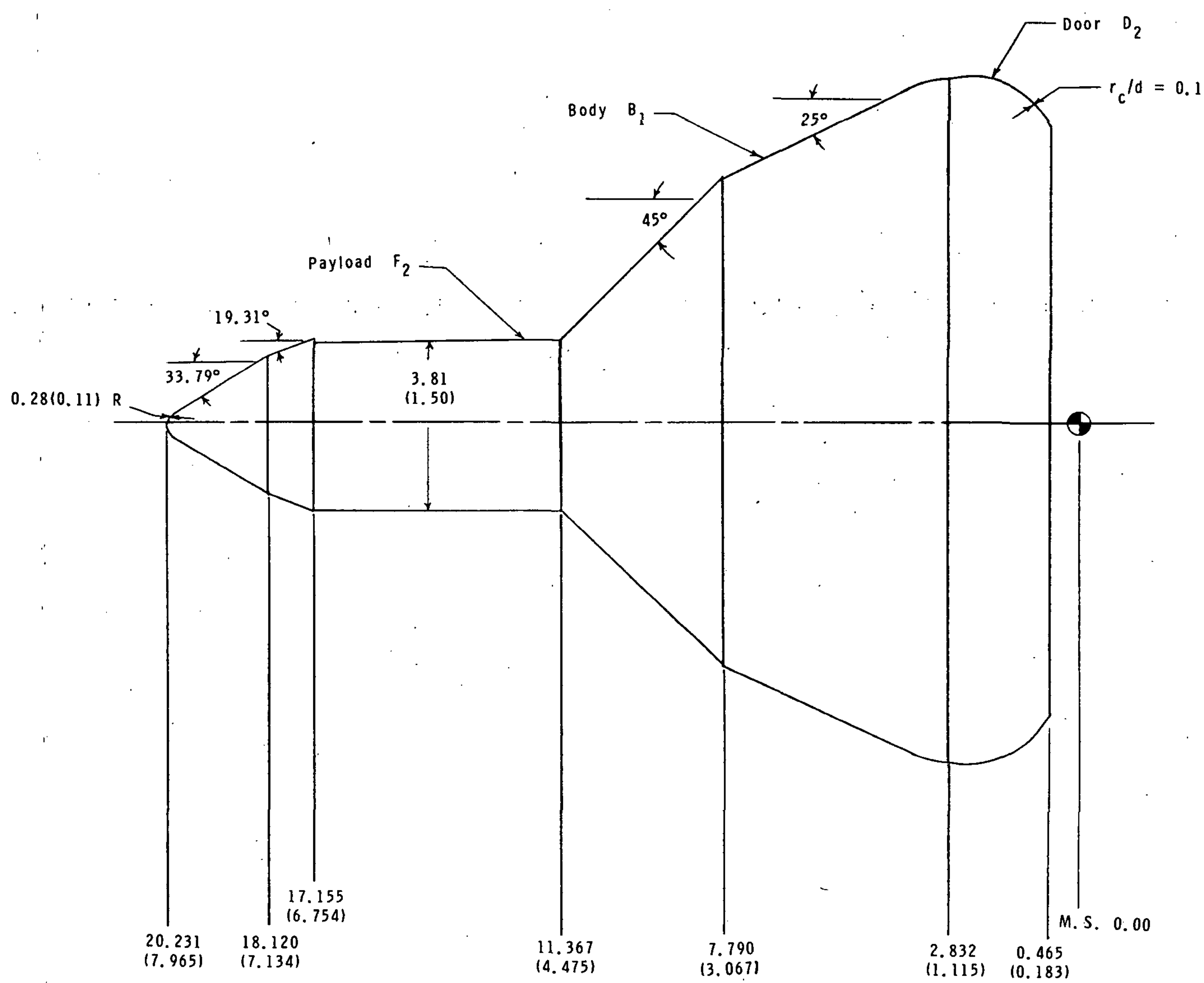

(b) Configuration 2 $(F_2B_1D_2)$.

Figure 1.- Continued.

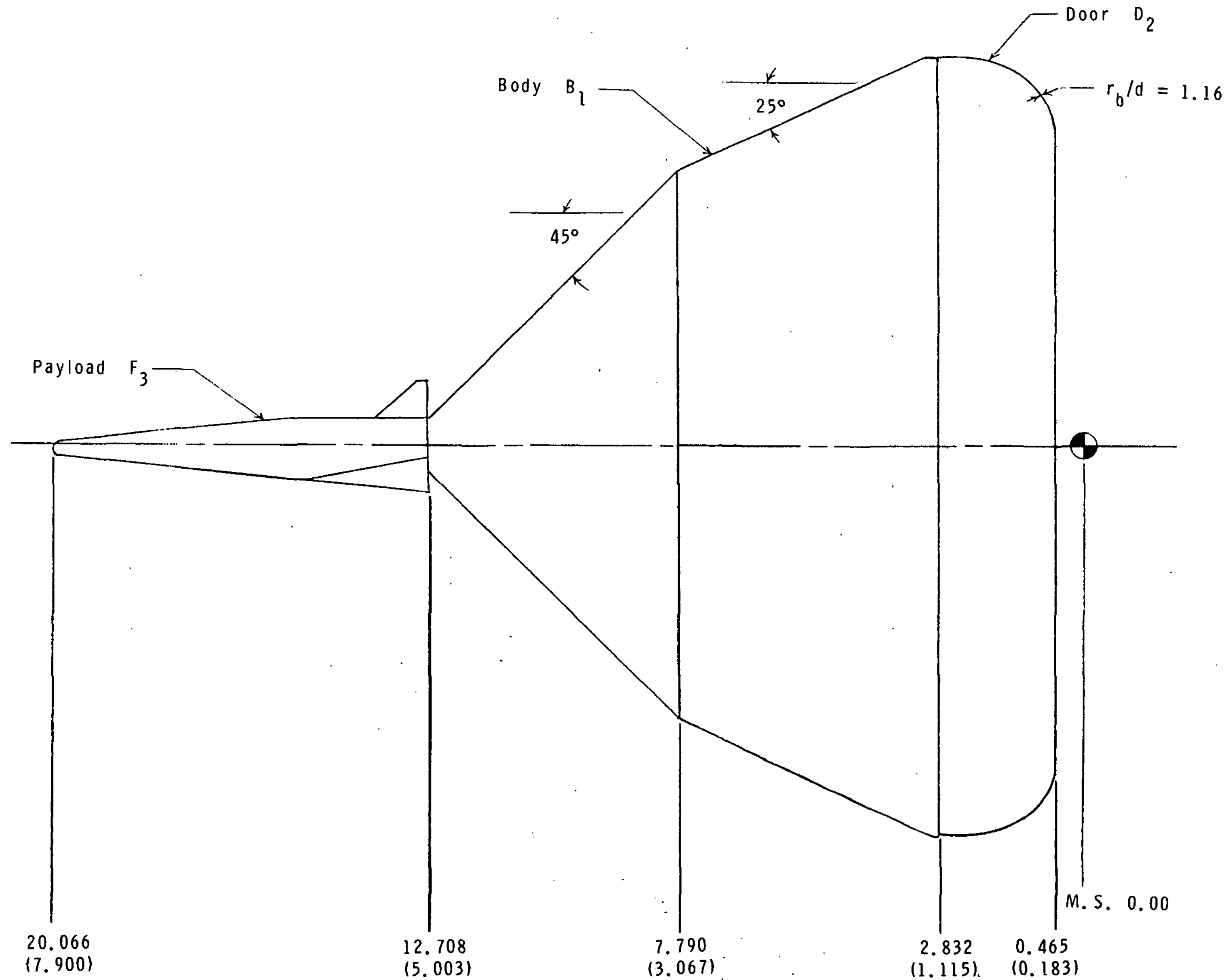

(c) Configuration 3 $(F_3B_1D_2)$.
Figure 1.- Continued.

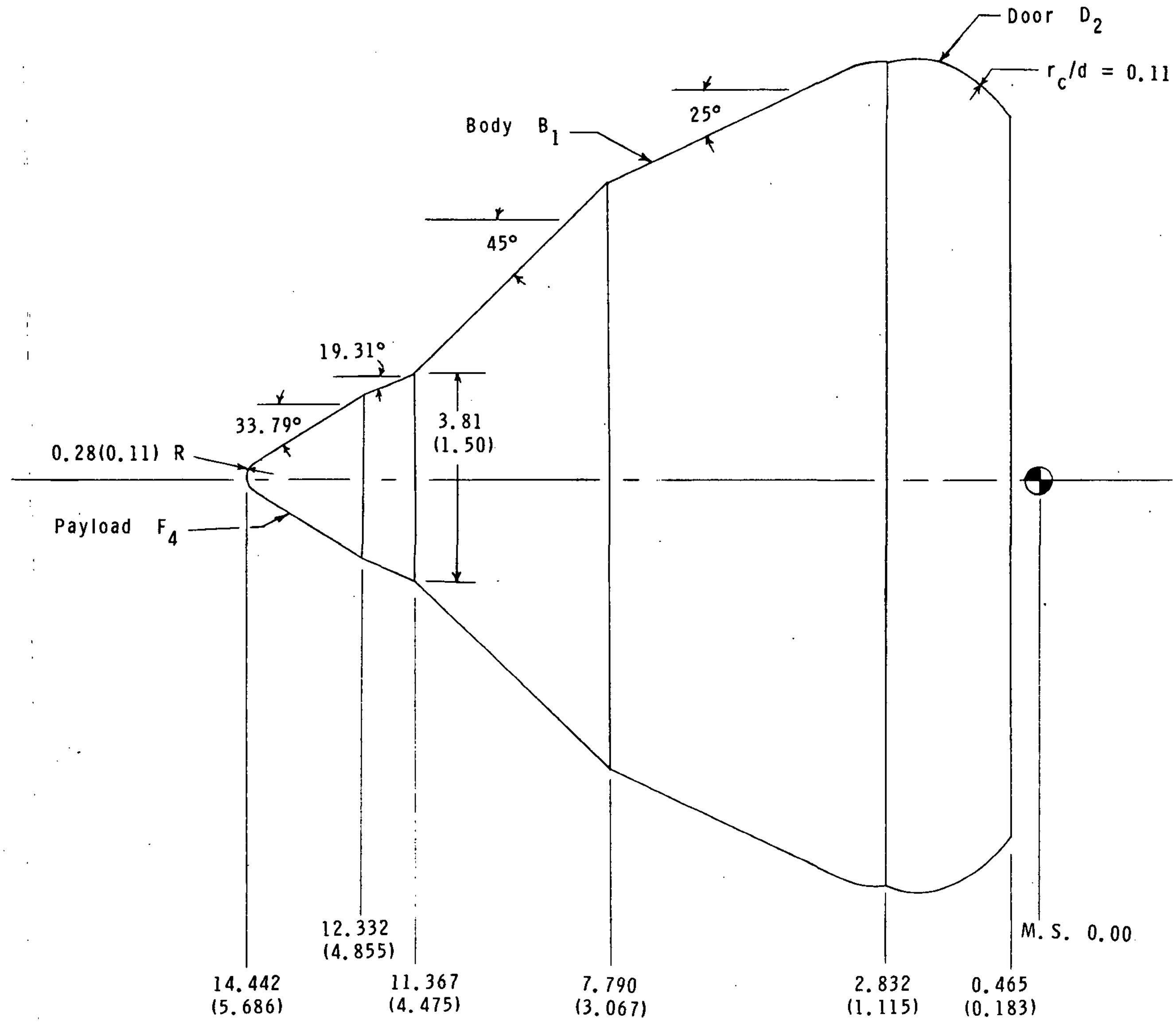

(d) Configuration 4 $(F_4B_1D_2)$.

Figure 1.- Continued.

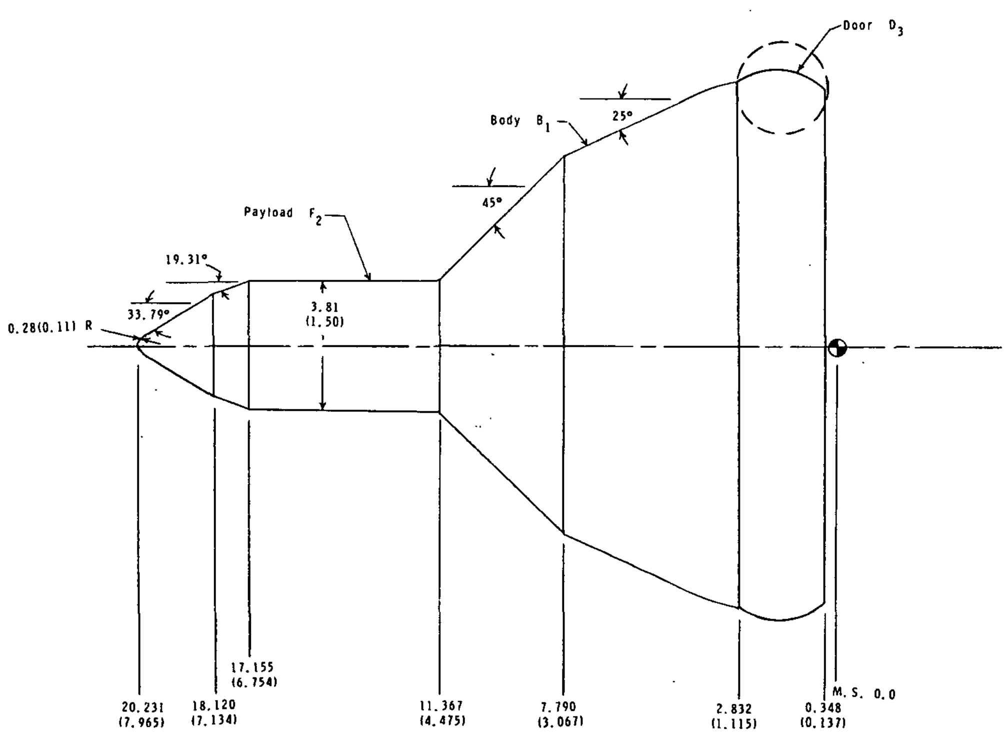

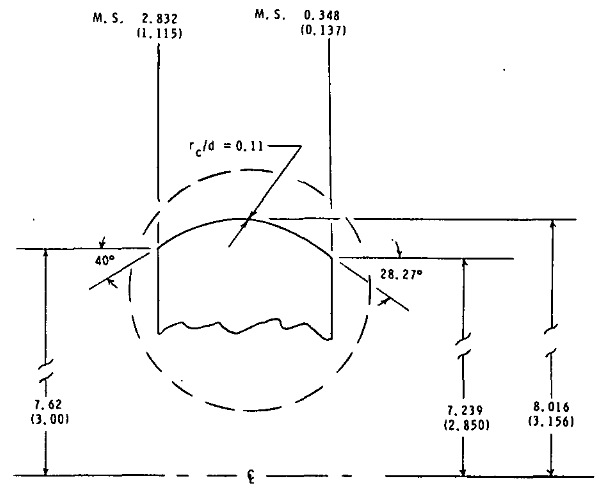

Details of engine door simulated open 45° (D_3)

(e) Configuration 5 $(F_2B_1D_3)$.

Figure 1.- Continued.

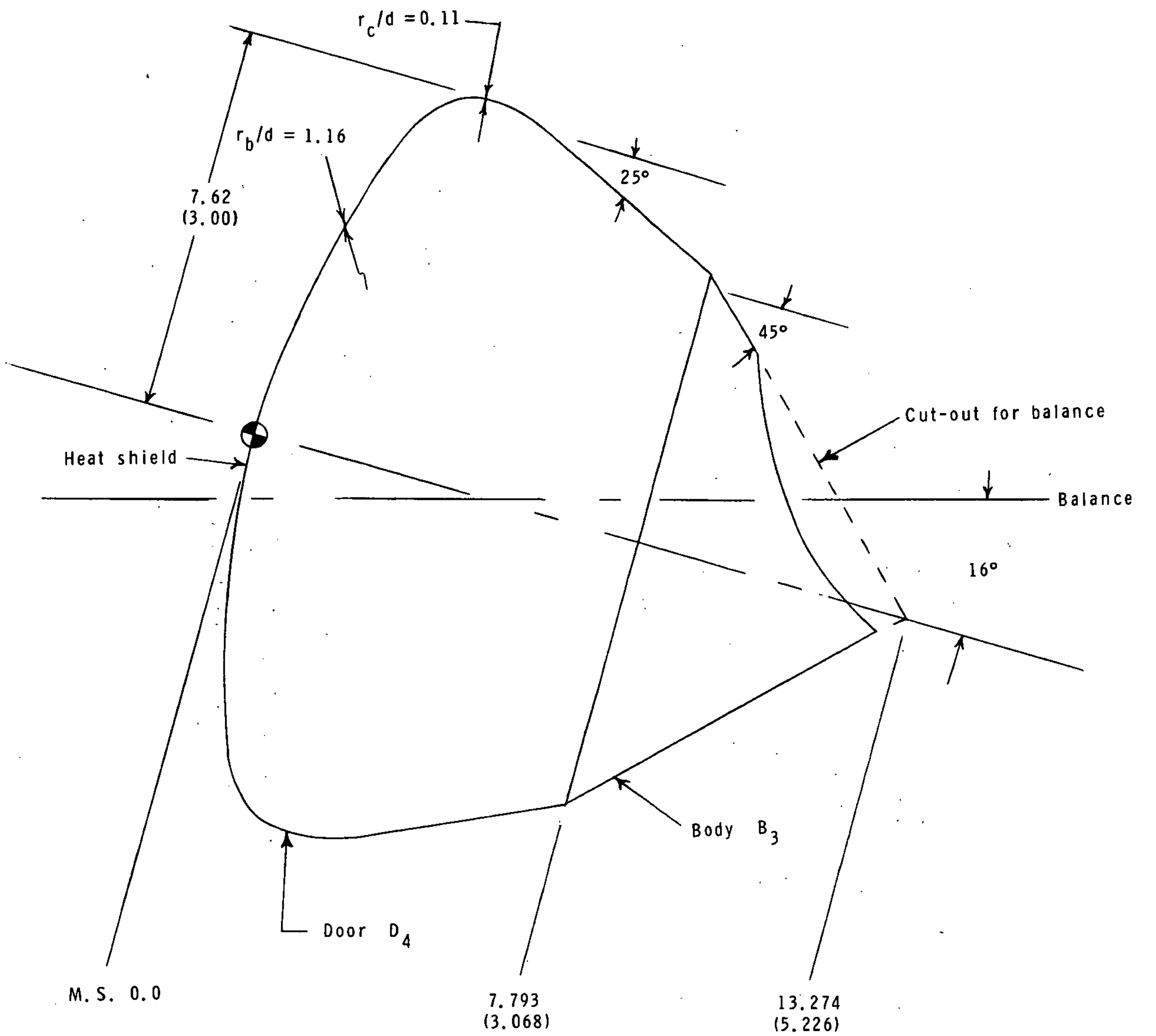

(f) Configuration 6 (OB_3D_4).

Figure 1.- Continued.

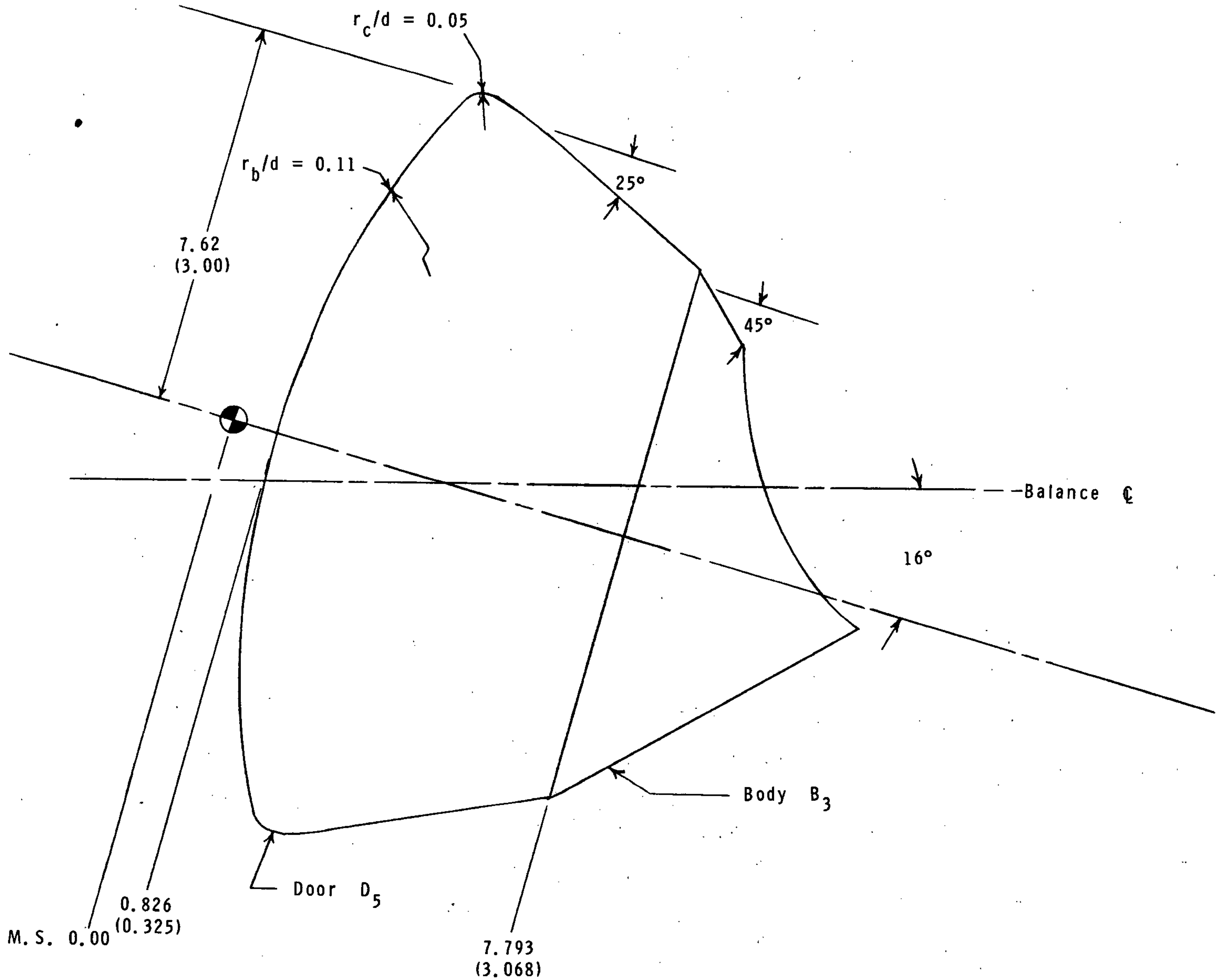

(g) Configuration 7 (OB_3D_5).

Figure 1.- Continued.

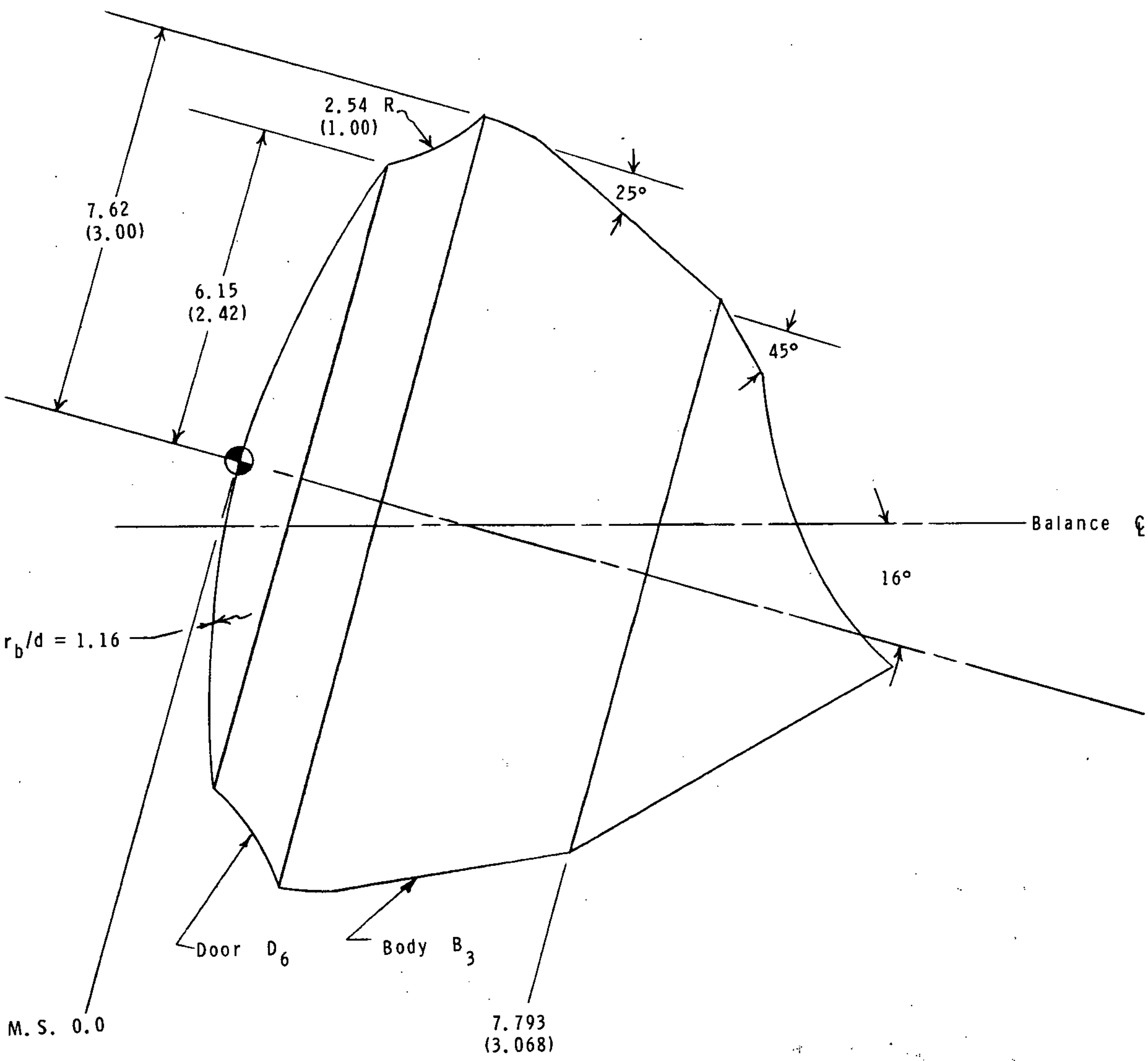

(h) Configuration 8 $\left(OB_3D_6\right)$.

Figure 1.- Continued.

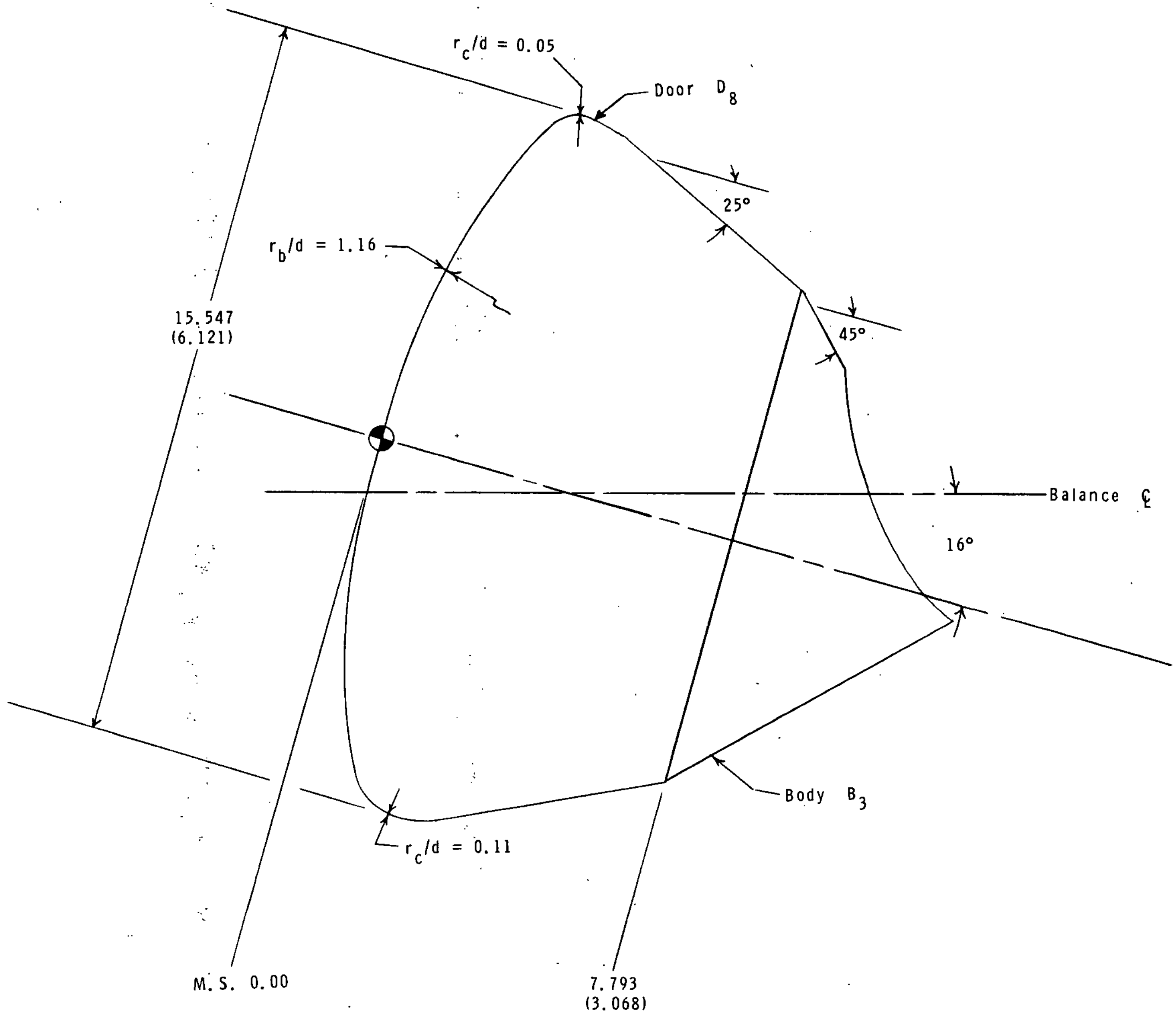

(i) Configuration 9 (OB_3D_8).

Figure 1.- Continued.

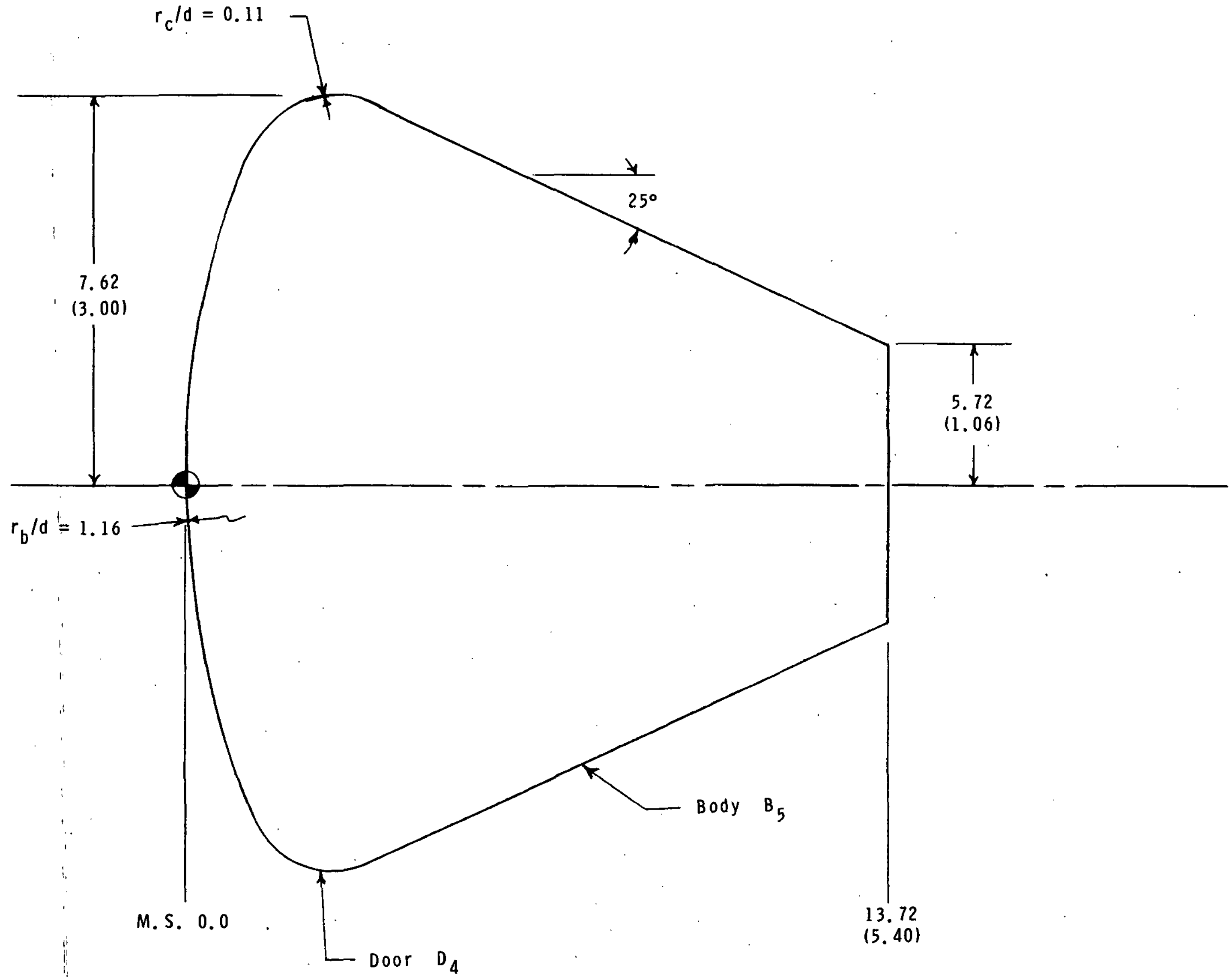

(j) Configuration 10 (OB_5D_4).

Figure 1.- Concluded.

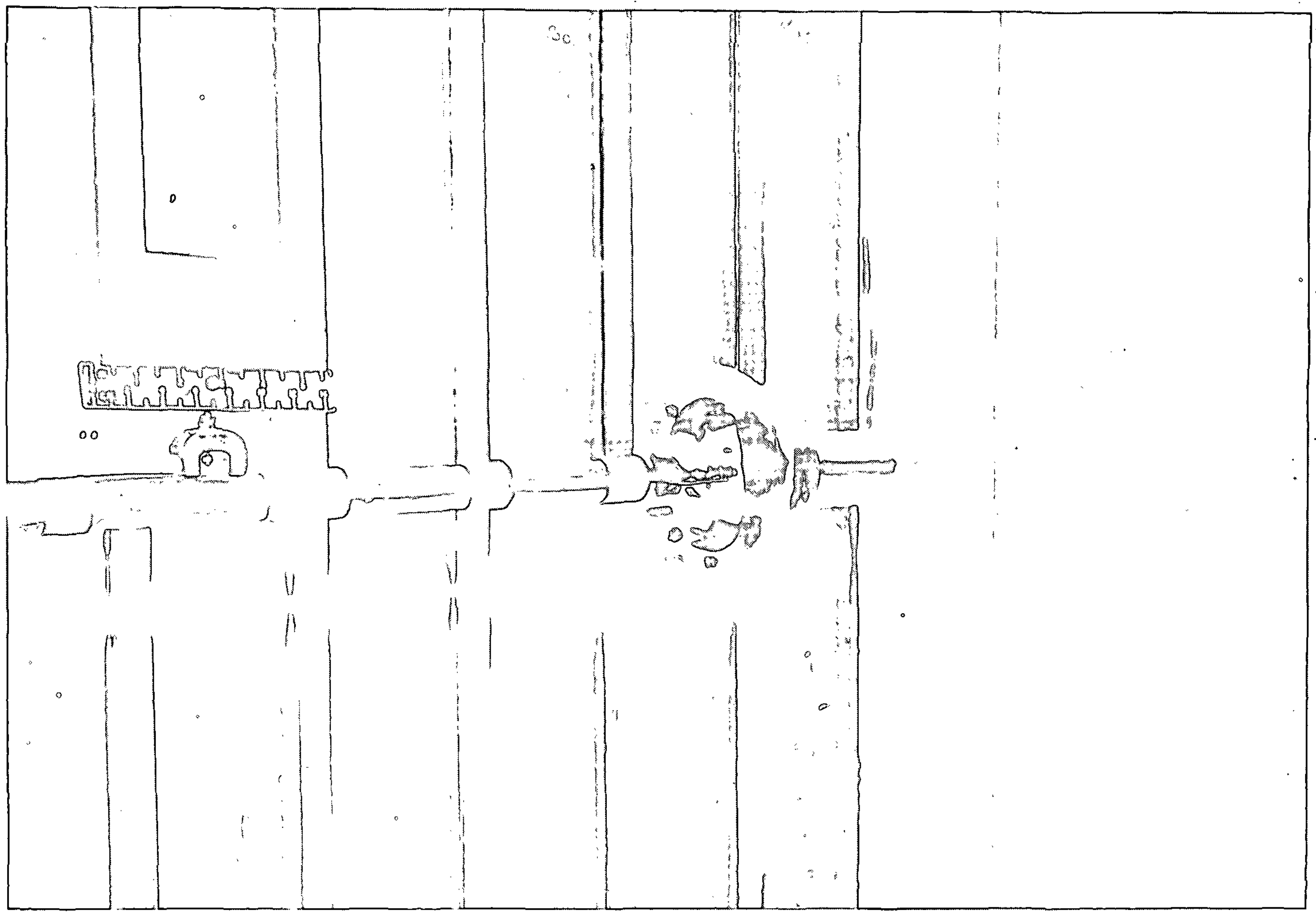

L-72-6549

(a) Configuration 1 $\left(F_1B_1D_2\right)$.

Figure 2.- Photographs of some test configurations.

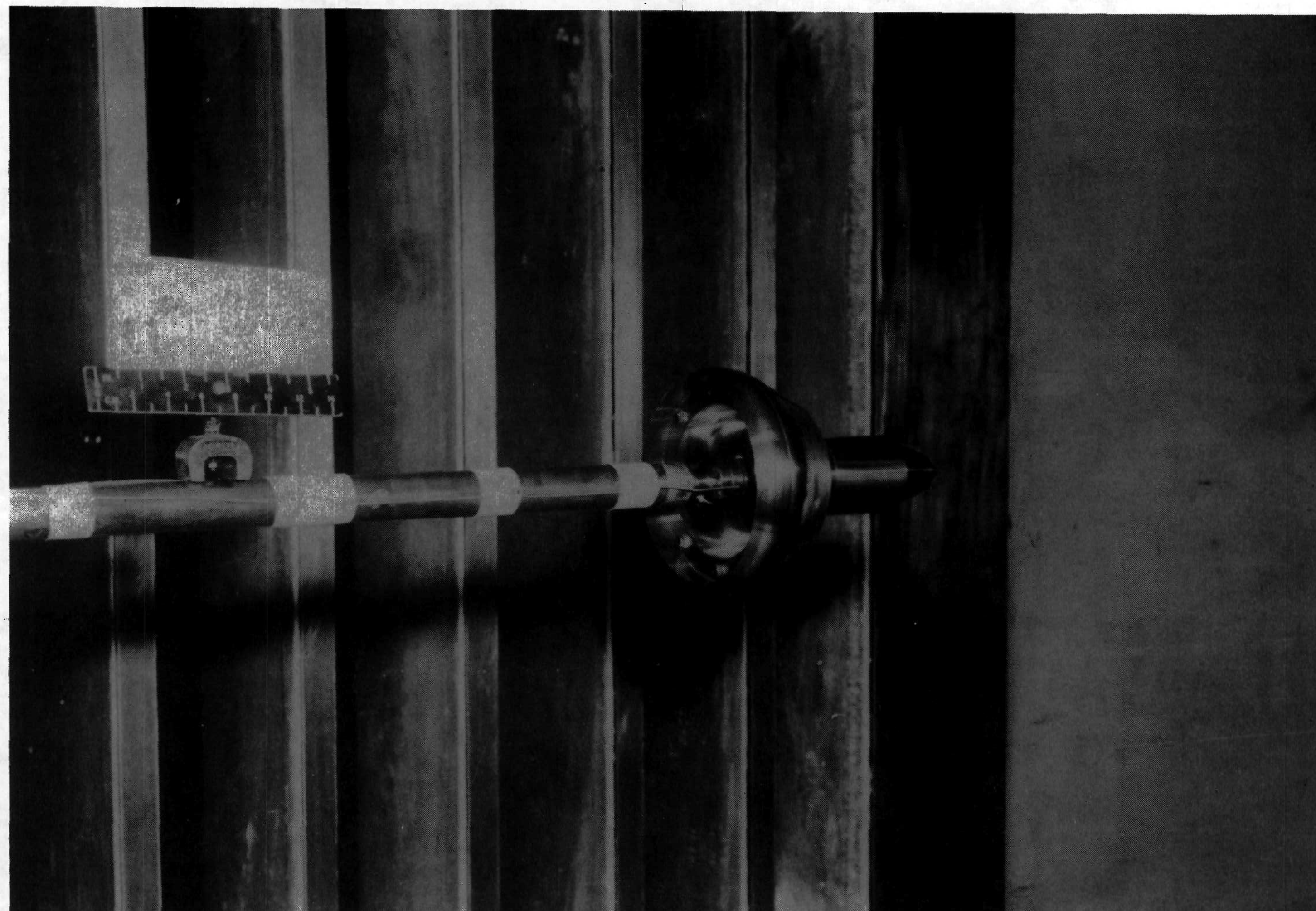

L-72-6549

(a) Configuration 1 $(F_1B_1D_2)$.

Figure 2.- Photographs of some test configurations.

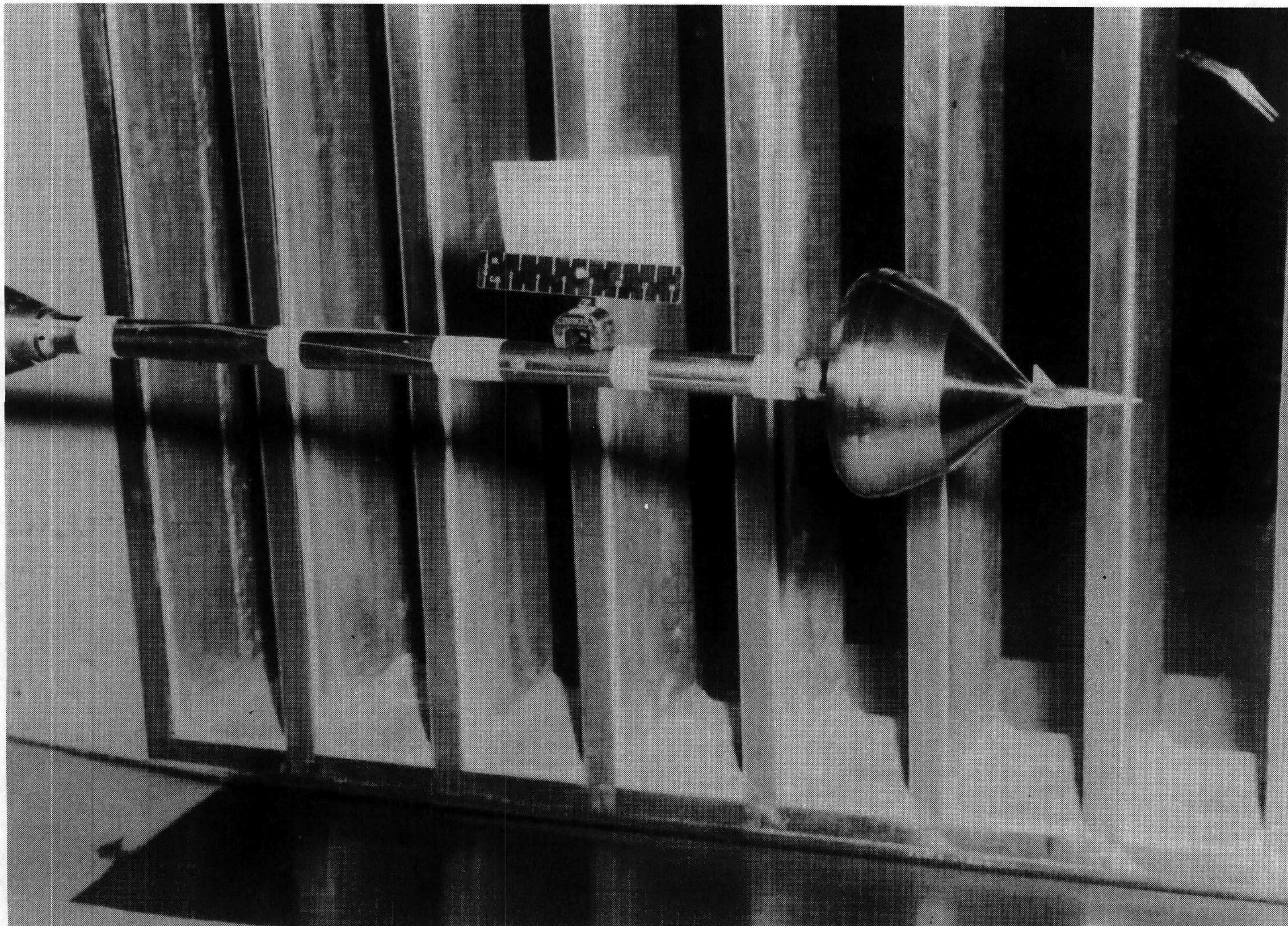

L-72-6550

(b) Configuration 3 $(F_3B_1D_2)$.

Figure 2.- Continued.

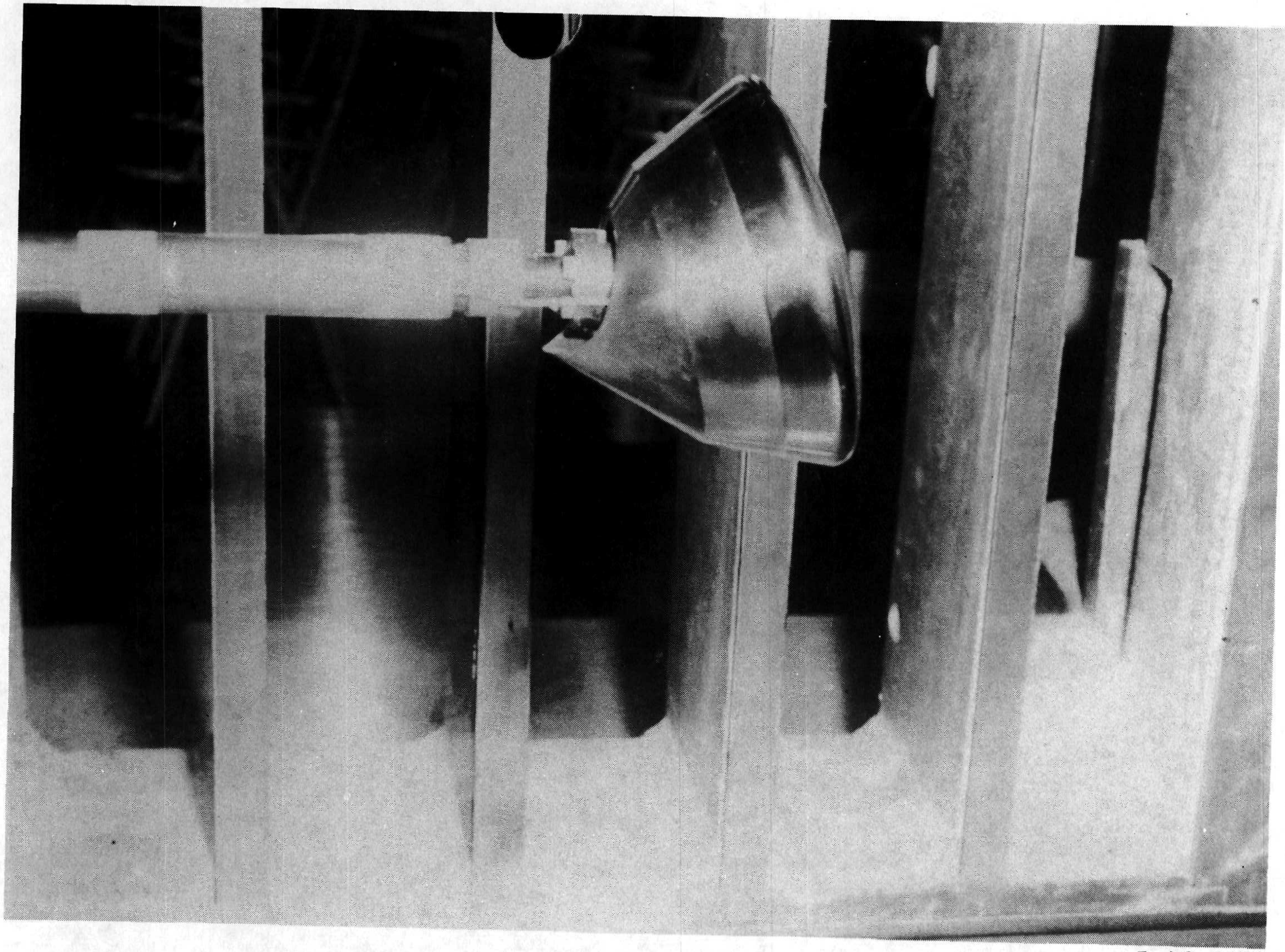

L-72-6551

(c) Configuration 7 (OB_3D_5).

Figure 2.- Continued.

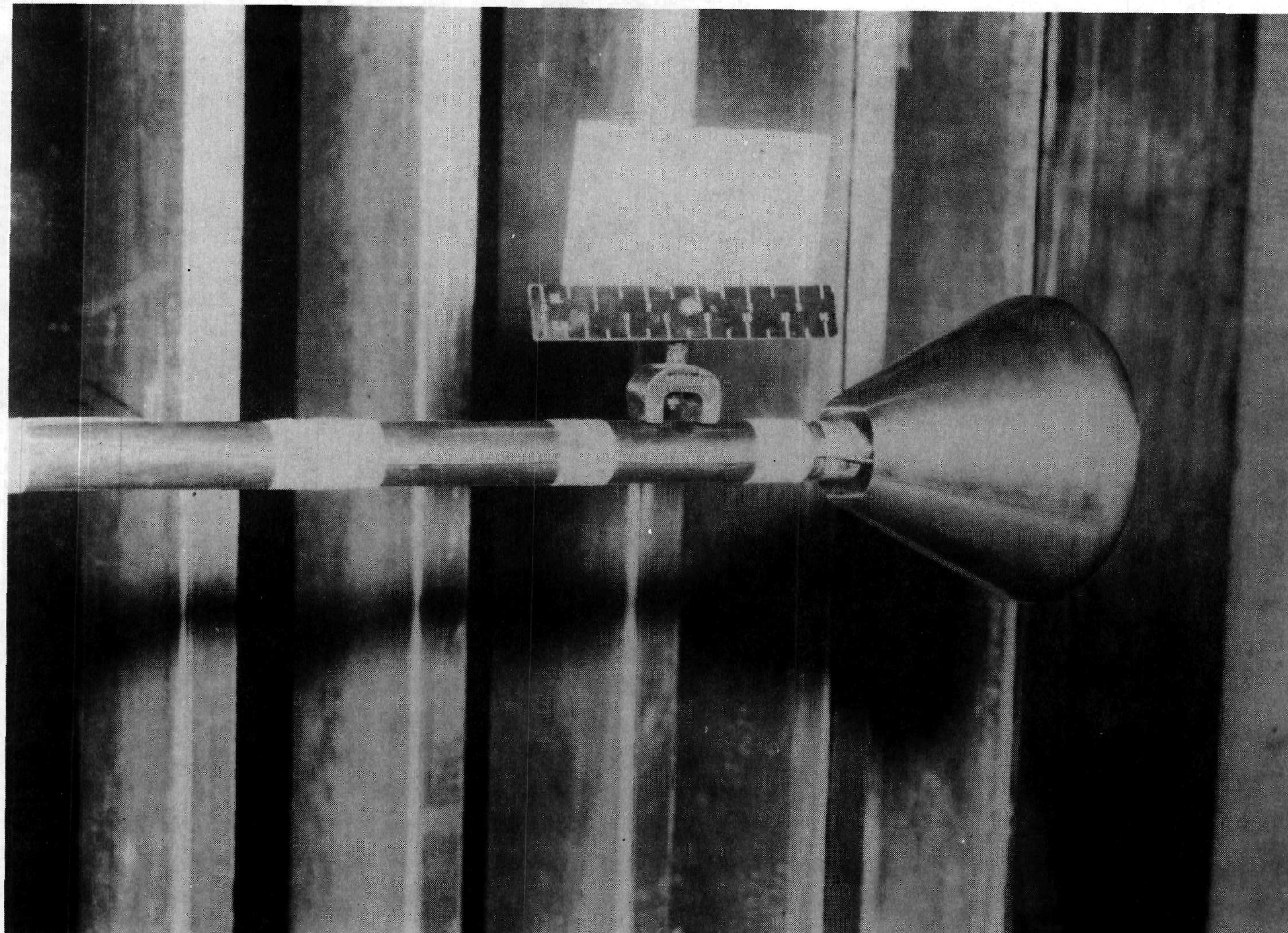

L-72-6552

(d) Configuration 10 (OB_5O_4).

Figure 2.- Concluded.

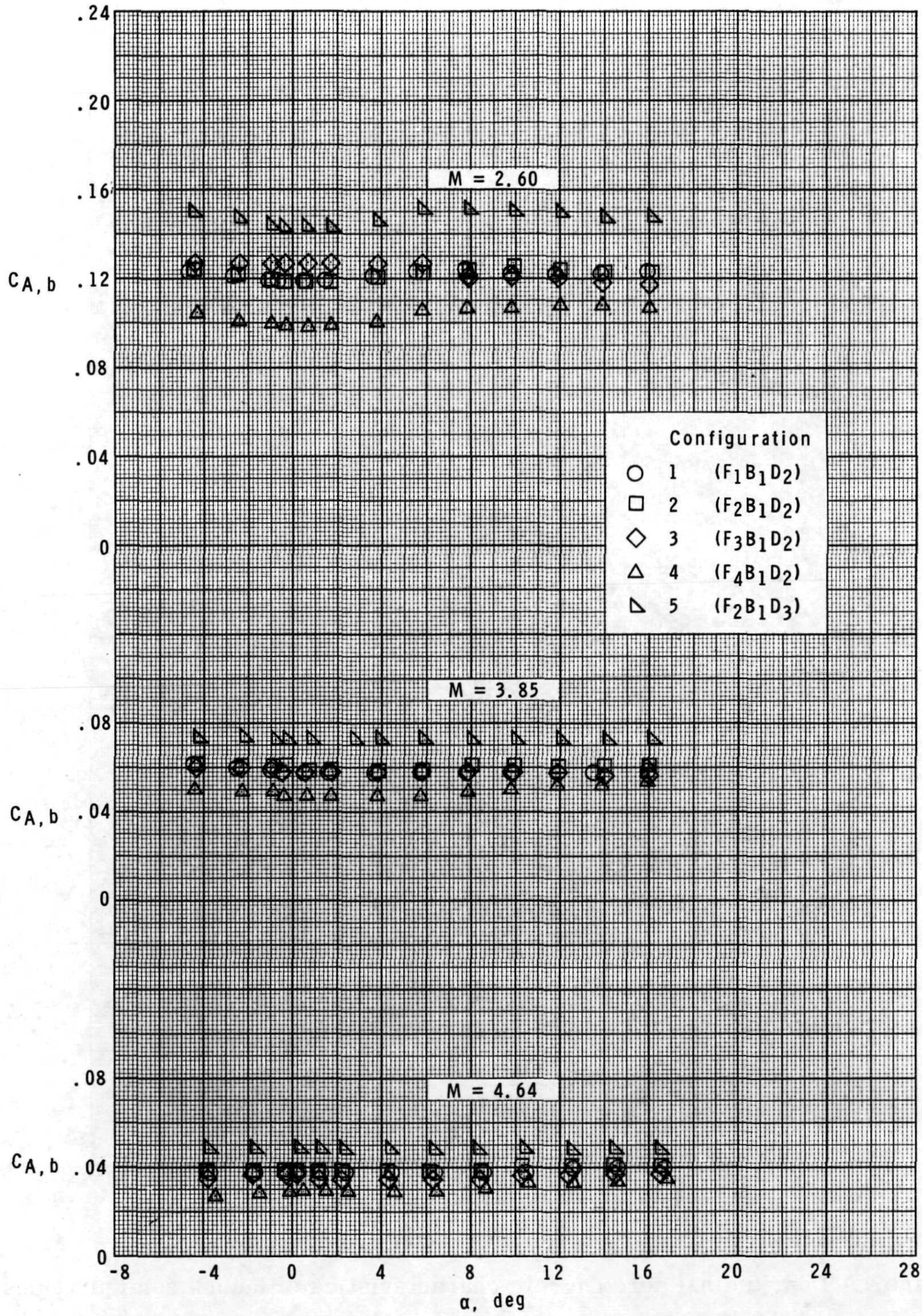

Figure 3.- Base axial-force coefficients for launch configurations.

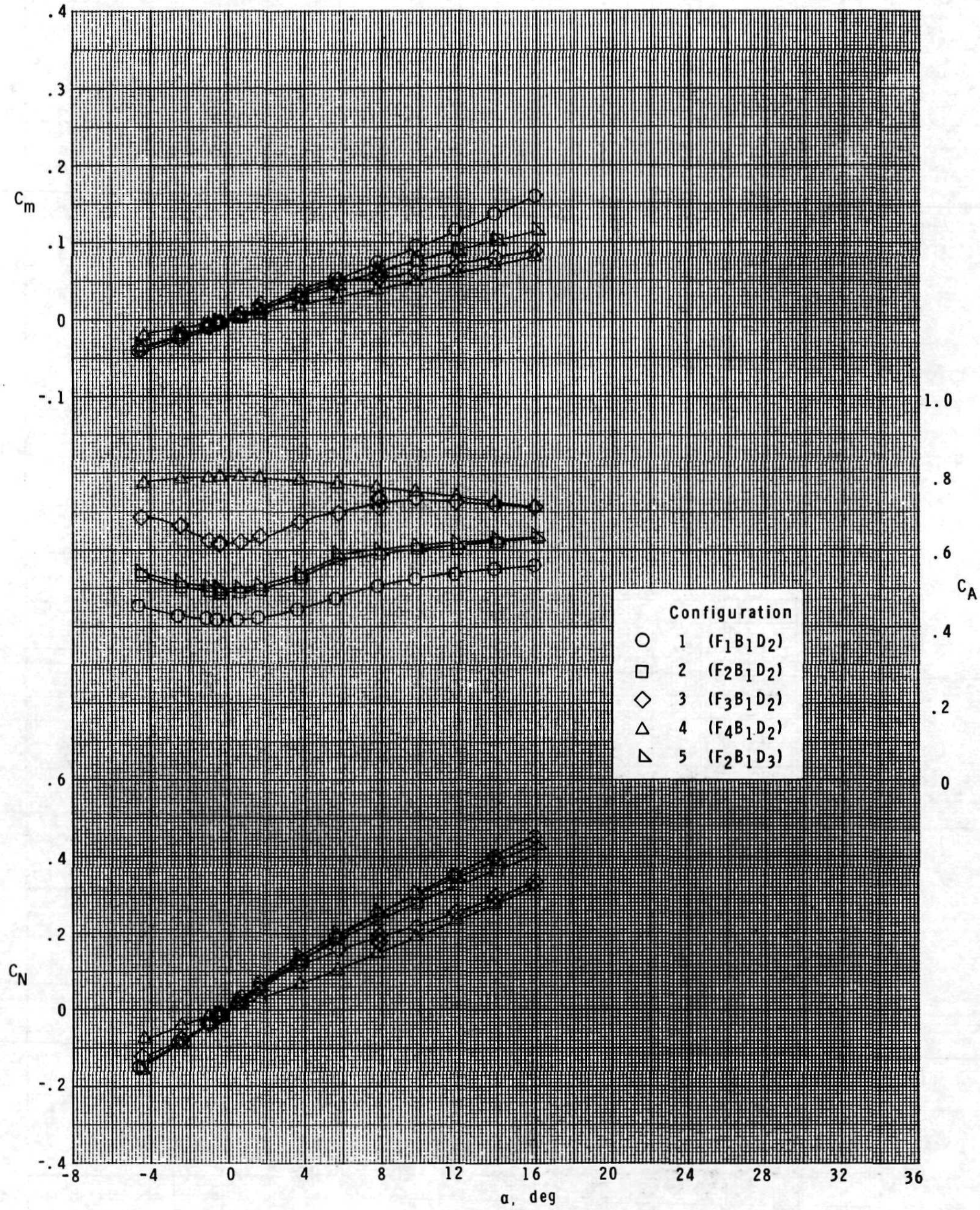

(a) M = 2.60.

Figure 4.- Longitudinal aerodynamic characteristics of launch configurations.

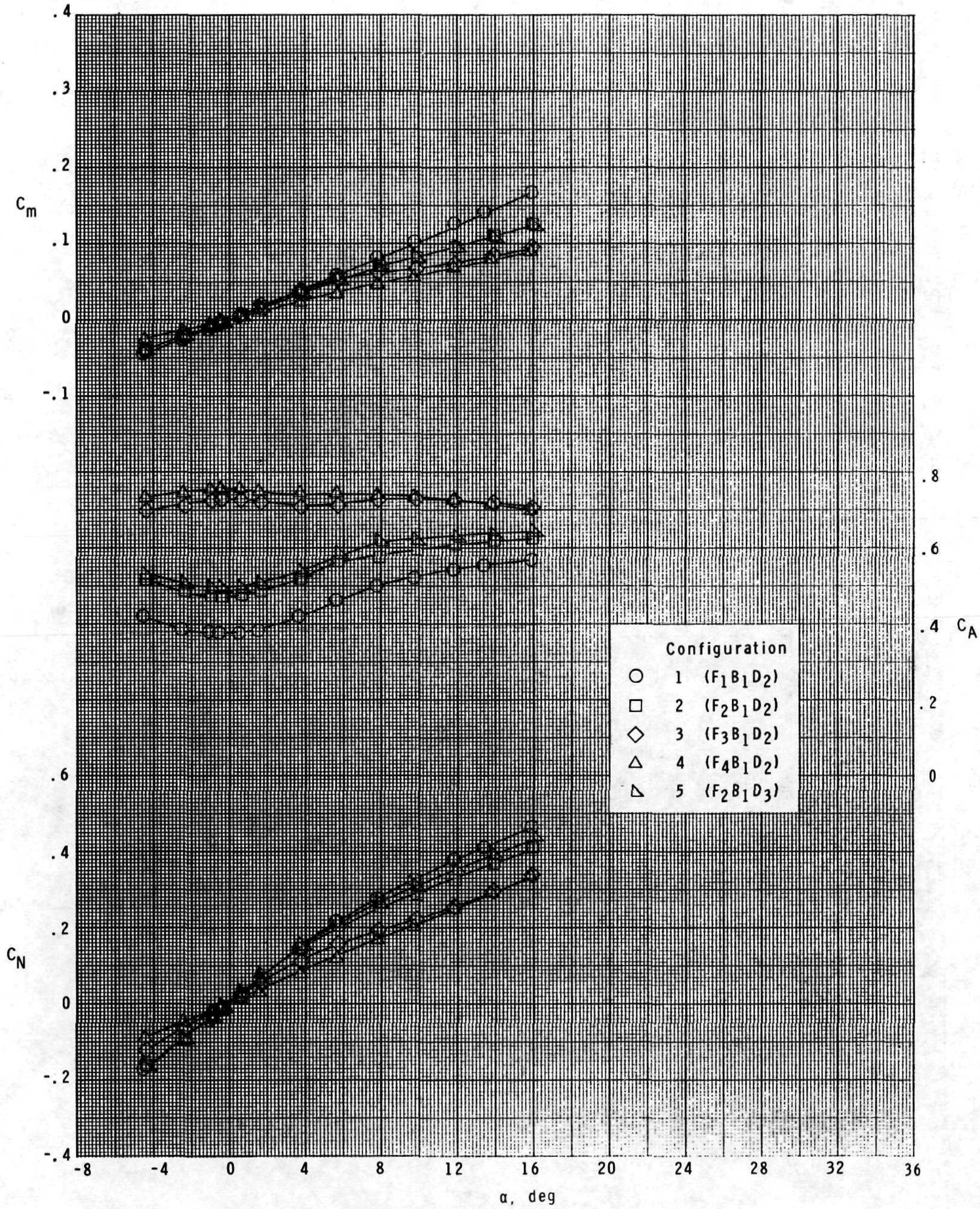

(b) M = 3.85.

Figure 4.- Continued.

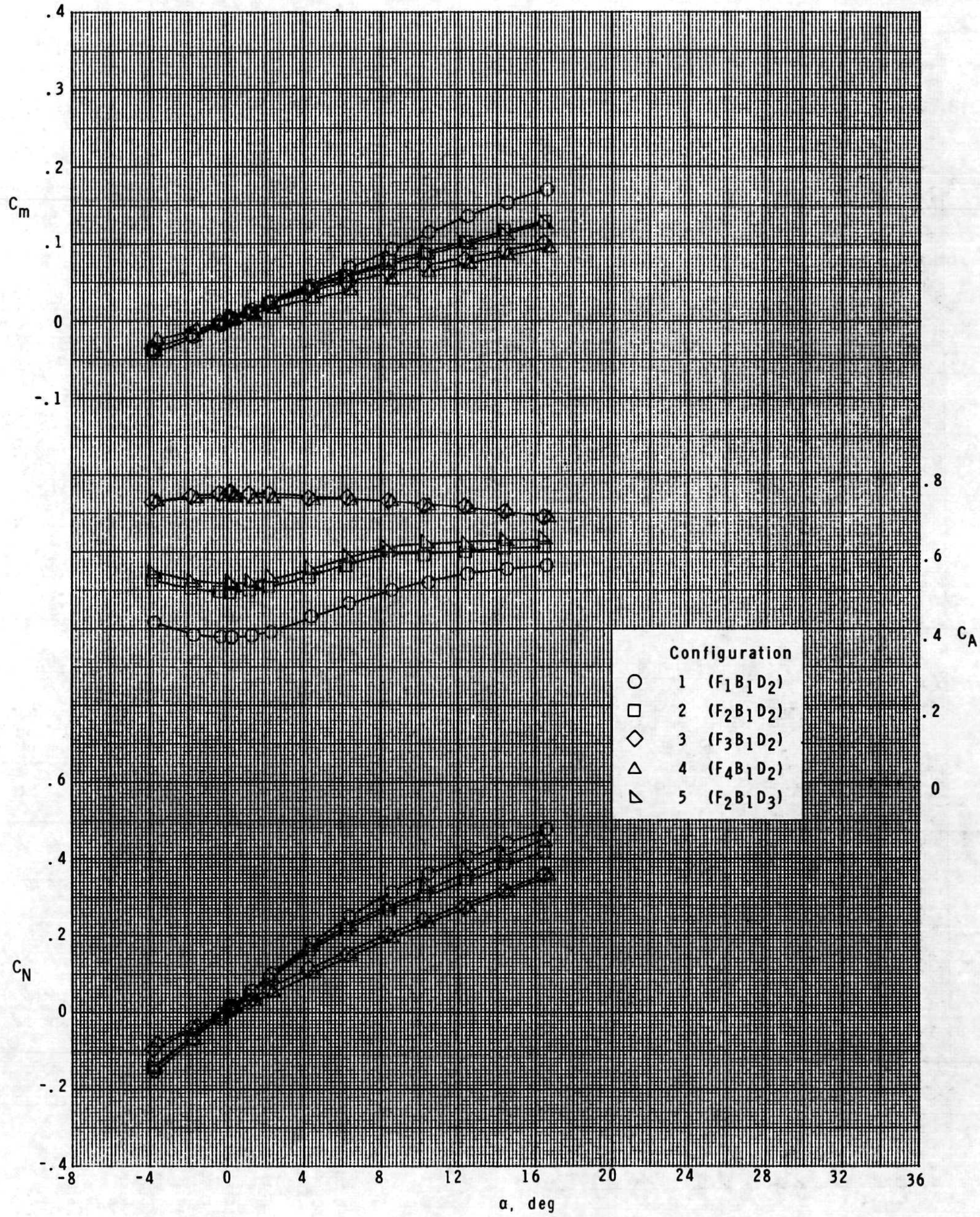

(c) M = 4.64.

Figure 4.- Concluded.

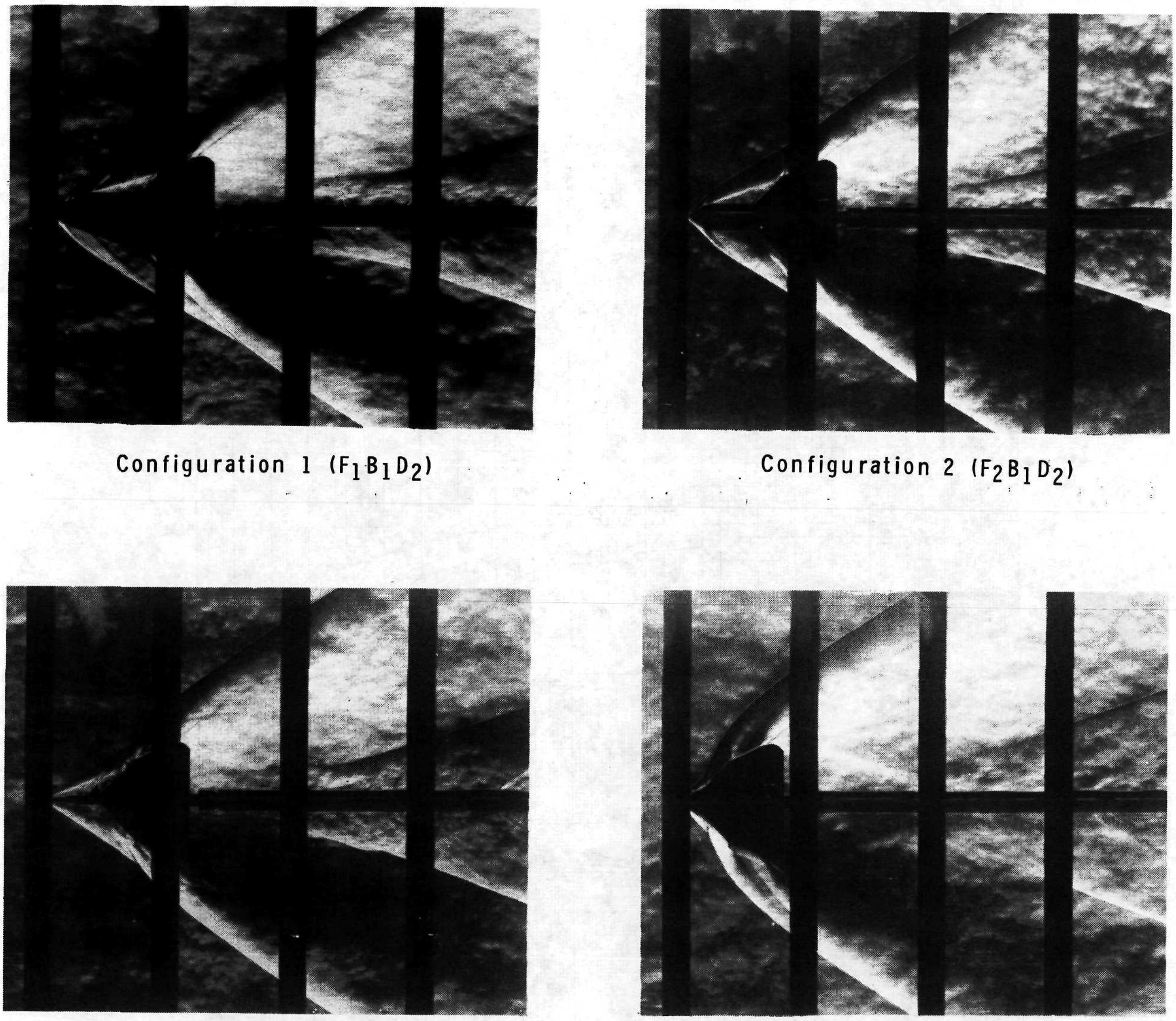

Configuration 1 ($F_1B_1D_2$)

Configuration 2 ($F_2B_1D_2$)

Configuration 3 ($F_3B_1D_2$)

Configuration 4 ($F_4B_1D_2$)

L-72-6553

Figure 5.- Schlieren photographs of some launch configurations. $M = 2.60$; $\alpha = 0^{\circ}$.

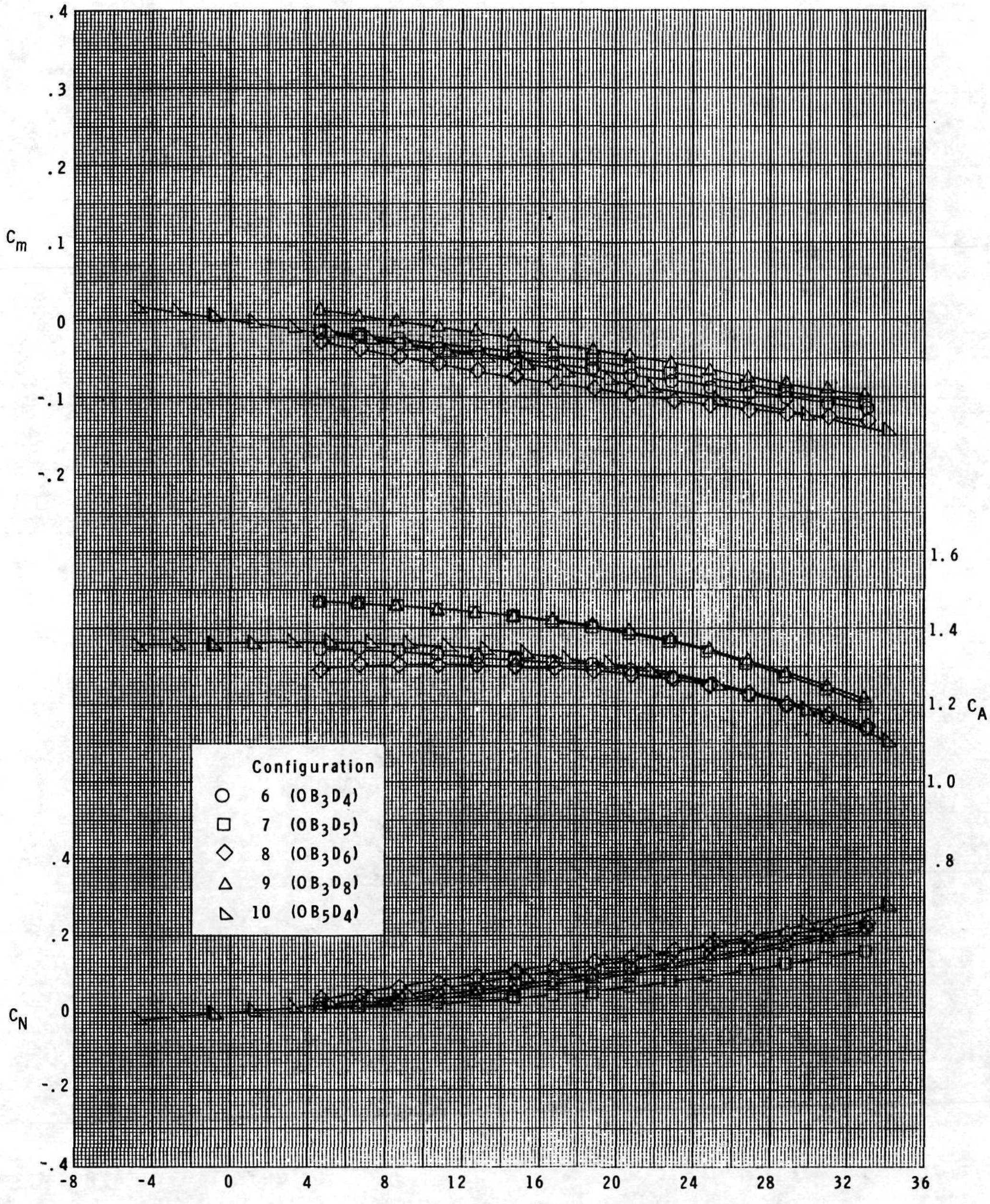

(a) M = 2.60.

Figure 6.- Longitudinal aerodynamic characteristics of entry configurations.

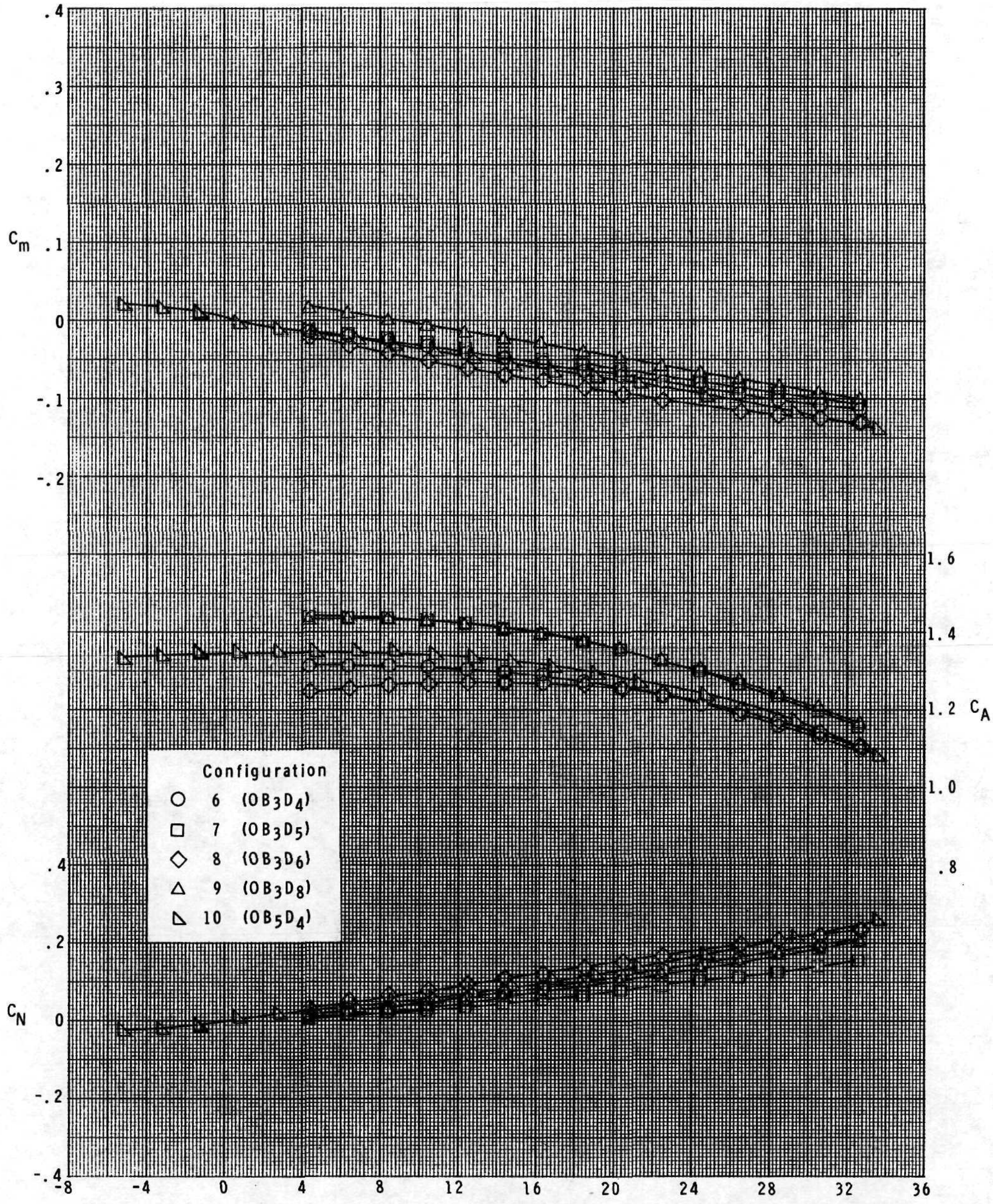

(b) M = 3.85.

Figure 6.- Continued.

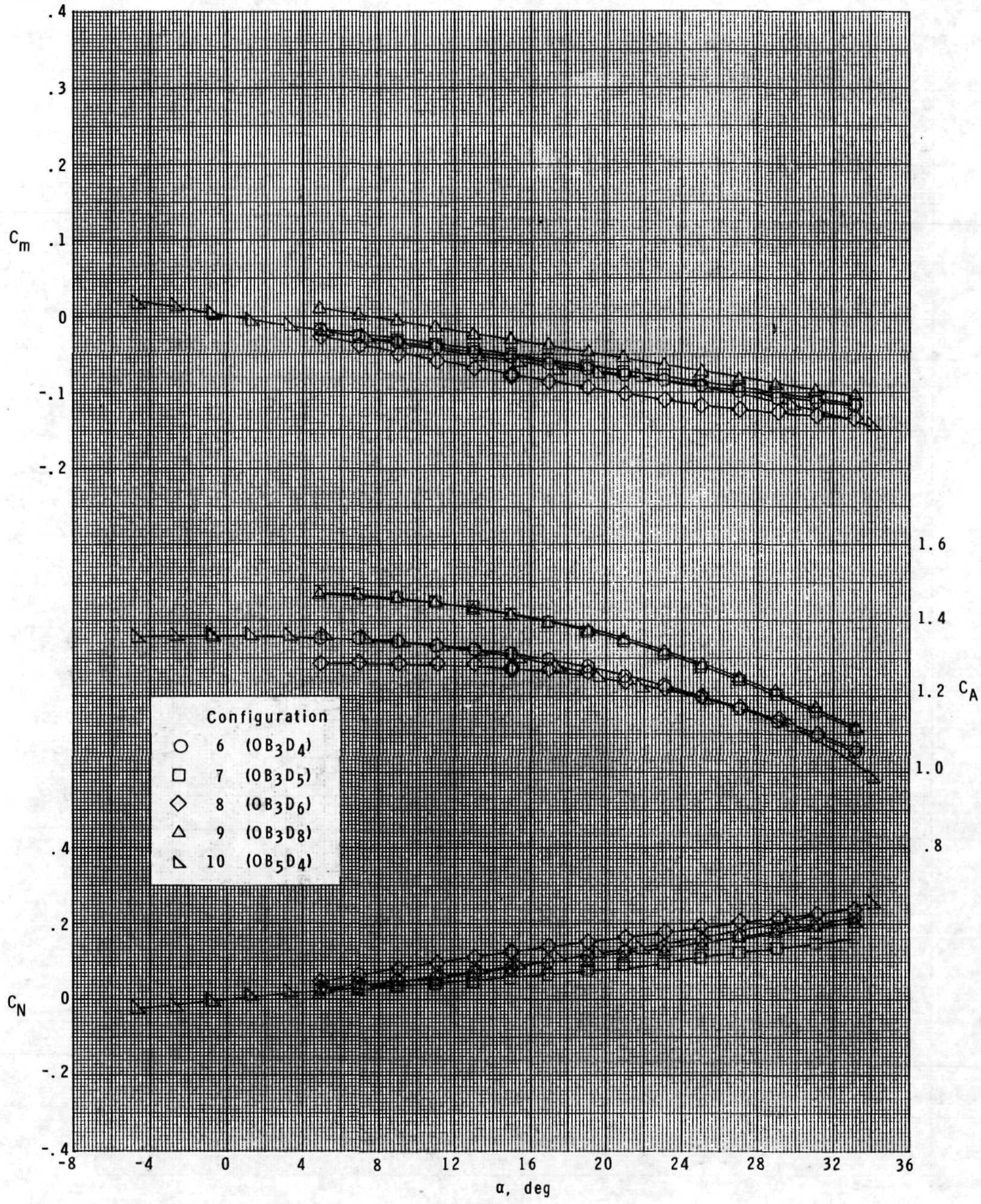

(c) M = 4.64.

Figure 6.- Concluded.

NASA-Langley, 1972 —— 31 L-8480

"The aeronautical and space activities of the United States shall be conducted so as to contribute . . . to the expansion of human knowledge of phenomena in the atmosphere and space. The Administration shall provide for the widest practicable and appropriate dissemination of information concerning its activities and the results thereof."

—NATIONAL AERONAUTICS AND SPACE ACT OF 1958

NASA SCIENTIFIC AND TECHNICAL PUBLICATIONS

TECHNICAL REPORTS: Scientific and technical information considered important, complete, and a lasting contribution to existing knowledge.

TECHNICAL NOTES: Information less broad in scope but nevertheless of importance as a contribution to existing knowledge.

TECHNICAL MEMORANDUMS: Information receiving limited distribution because of preliminary data, security classification, or other reasons. Also includes conference proceedings with either limited or unlimited distribution.

CONTRACTOR REPORTS: Scientific and technical information generated under a NASA contract or grant and considered an important contribution to existing knowledge.

TECHNICAL TRANSLATIONS: Information published in a foreign language considered to merit NASA distribution in English.

SPECIAL PUBLICATIONS: Information derived from or of value to NASA activities. Publications include final reports of major projects, monographs, data compilations, handbooks, sourcebooks, and special bibliographies.

TECHNOLOGY UTILIZATION PUBLICATIONS: Information on technology used by NASA that may be of particular interest in commercial and other non-aerospace applications. Publications include Tech Briefs, Technology Utilization Reports and Technology Surveys.

Details on the availability of these publications may be obtained from:

SCIENTIFIC AND TECHNICAL INFORMATION OFFICE

NATIONAL AERONAUTICS AND SPACE ADMINISTRATION

Washington, D.C. 20546